MNRAS 000, 1–13 (2022) Preprint 22 April 2022 Compiled using MNRAS LATEX style file v3.0

An Hα survey of the host environments of 77 type IIn supernovae within $z < 0.02$

C. L. Ransome,[1, 2]★ S. M. Habergham-Mawson[1], M. J. Darnley[1], P. A. James[1] and S. M. Percival[1]

[1]*Astrophysics Research Institute, Liverpool John Moores University, Liverpool Science Park iC2, Liverpool, Merseyside, L3 5RF, UK*
[2]*Isaac Newton Group of Telescopes, Edificio Mayantigo, Calle Alvarez Abreu, 70, 2 piso, E-38700 Santa Cruz de La Palma, Canary Islands, Spain*

Accepted XXX. Received YYY; in original form ZZZ

ABSTRACT

Type IIn supernovae (SNe IIn) are an uncommon and highly heterogeneous class of SN where the SN ejecta interact with pre-existing circumstellar media (CSM). Previous studies have found a mass ladder in terms of the association of the SN location with Hα emission and the progenitor masses of SN classes. In this paper, we present the largest environmental study of SNe IIn. We analyse the Hα environments of 77 type IIn supernovae using continuum subtracted Hα images. We use the pixel statistics technique, normalised cumulative ranking (NCR), to associate SN pixels with Hα emission. We find that our 77 SNe IIn do not follow the Hα emission. This is not consistent with the proposed progenitors of SNe IIn, luminous blue variables (LBVs) as LBVs are high mass stars that undergo dramatic episodic mass loss. However, a subset of the NCR values follow the Hα emission, suggesting a population of high mass progenitors. This suggests there may be multiple progenitor paths with ~60% having non-zero NCR values with a distribution consistent with high mass progenitors such as LBVs and ~40% of these SNe not being associated with Hα emission. We discuss the possible progenitor routes of SNe IIn, especially for the zero NCR value population. We also investigate the radial distribution of the SNe in their hosts in terms of Hα and r'-band flux.

Key words: supernovae:general – stars:circumstellar material

1 INTRODUCTION

1.1 Type IIn supernovae

First categorised by Filippenko (1989, as Seyfert I SNe) and Schlegel (1990), type IIn supernovae (SNe IIn) account for around 7% of the total SN population (Li et al. 2011). SNe IIn are generally spectroscopically characterised by a narrow feature on the Balmer series (most obvious on the Hα line) with full width half-maximum (FWHM) $\sim 10^2$ km s^{-1} (Filippenko 1997). This narrow feature is superimposed on an intermediate width (FWHM $\sim 10^3$ km s^{-1}) and/or a broad component (FWHM $\sim 10^{3-4}$ km s^{-1}). These characteristic narrow features originate from the SN ejecta shocking pre-existing, dense, cold, and slow circumstellar medium (CSM) with CSM densities $\sim 10^{-13}$–10^{-15} gcm^{-3} (Yaron et al. 2017). A Hα excess is created when emission from this interaction ionises the surrounding, unshocked, CSM and then recombines (Chugai 1991; Chugai et al. 2004). The broader components originate from the SN ejecta. The intermediate components may originate from interaction with a massive and dense, clumpy wind Chugai et al. (2004), possibly further broadened by Thompson scattering (Chugai 2001; Dessart et al. 2009; Humphreys et al. 2012; Huang & Chevalier 2018). SNe IIn often lack the P-Cygni features seen in other SN classes (with exceptions such as SN 2012ab Gangopadhyay et al. 2020) and have a blue continuum which may originate from the strong CSM interaction (Stathakis & Sadler 1991; Turatto et al. 1993).

The CSM surrounding a SN IIn progenitor comes from the progenitor itself or, in some cases, a companion star. The progenitor may experience mass loss episodes toward the end of its life (Smith 2014). Using light curve modelling, Moriya et al. (2014) found that the mass loss rate of SN IIn progenitors may exceed 10^{-3} M$_\odot$ yr^{-1} in the decades preceding the SN explosion. In their final moments, the mass loss may be more eruptive and dramatic (Ofek et al. 2014; Strotjohann et al. 2021). This is apparent in transients such as SN 2009ip (Mauerhan & Smith 2012; Smith et al. 2014) where the initial eruptions were non-terminal explosions sometimes known as a SN impostor. However, in the case of SN 2009ip, the nature of the final 2012 eruption is debated. Pastorello et al. (2013) found that the spectrum of SN 2009ip showed high ejecta velocities (~ 13,000 kms^{-1}) between the 2009 eruption and the possible terminal 2012 events, showing that these velocities do not preclude a CCSN. Instead, Pastorello et al. suggest that the spectrum of the September 2012 eruption was similar to the September 2011 and Au-

★ E-mail: C.Ransome@2018.ljmu.ac.uk

gust 2012 eruptions. Those authors suggest that SN 2009ip may have undergone a non-terminal pair-instability event. Other non-terminal scenarios for SN 2009ip are described by Fraser et al. (2013) and Fraser et al. (2015), and Elias-Rosa et al. (2018) found that the SN impostor, SNhunt 151 was remarkably similar to SN 2009ip, those authors suggest that may be an η Car-like LBV "great" eruption that occur in a dense CSM. However subsequent, late-time observations suggest that the final eruption of SN 2009ip was terminal (e.g. Graham et al. 2017). Furthermore, SN 2011fh similarly underwent SN 2009ip-like mass loss events prior to its death as a SN and may have had a massive progenitor based on the parent cluster age of $\sim$4.5 Myr (Pessi et al. 2021). Some of these impostor events may originate from the eruptive mass loss episodes from luminous blue variable (LBV) progenitor (Mauerhan et al. 2013; Ofek et al. 2014; Pastorello et al. 2018). CSM may also be created by super asymptotic giant branch (AGB) progenitors or companions through massive winds.

SNe IIn are a heterogeneous SN class. Some SNe IIn are generally more luminous, reaching superluminous luminosities (e.g., SN 2006gy with an absolute magnitude of –22, Ofek et al. 2007; Smith et al. 2007). Some SNe IIn are also very long lived, remaining bright for years post-explosion (e.g., SN 1988Z, SN 2005ip, SN 2010jl and SN 2015da; Stathakis & Sadler 1991; Turatto et al. 1993; Filippenko 1997; Stritzinger et al. 2012; Smith et al. 2016, 2017; Tartaglia et al. 2020). Therefore, SNe IIn display a wide locus over the timescale-luminosity phase space of exploding transients (Kasliwal et al. 2011). Some SNe IIn, unlike their superluminous counterparts, inhabit the standard core-collapse SN (CCSN) phase-space with absolute magnitudes between –17 and –19 (Li et al. 2011; Kiewe et al. 2012; Taddia et al. 2013). Additionally, Nyholm et al. (2020) reported a SN IIn light curve rise time bimodality; with a population of slow risers, and a separate population of fast risers. Such diversity may be explained by considering that SNe IIn may have multiple progenitor paths.

1.2 Progenitor systems of type IIn supernovae

1.2.1 *Massive progenitors*

LBVs may be considered a transitional phase in the life of a massive star where an O-type star sheds its outer H-rich layer and becomes a Wolf-Rayet (WR) star (Humphreys & Davidson 1994; Weis & Bomans 2020). LBVs may expel material through massive winds and more dramatic episodic eruptions. The mass loss rates from eruptive episodes, such as the great eruption of η Car in the 19th century, can be as high as $1\,M_\odot\,yr^{-1}$, which can lead to ejected envelopes with masses as high as $10\,M_\odot$ (Smith et al. 2003, 2010). LBVs are observed progenitors of at least one SN IIn, SN 2005gl in NGC 266 (Gal-Yam et al. 2007).

While LBVs can have masses in excess of $50\,M_\odot$, Groh et al. (2013b) found that LBVs may arise from more intermediate mass stars with masses between $20-25\,M_\odot$. Groh et al. report that after a red supergiant (RSG) phase, the pre-SN spectra in their simulations were consistent with the spectra of LBVs. Ofek et al. (2014), using SNe IIn from the Palomar Transient Survey (Law et al. 2009; Rau et al. 2009) found that half of SNe IIn in the sample had precursor events resulting in an increase in brightness prior to the SN explosion that the authors interpret as outbursts. Indeed, the progenitor of SN 2010mc suffered large eruptive mass loss only 40 days before the SN explosion (Ofek et al. 2013).

There remains a question as to whether LBVs can directly end their lives as SNe. In contrast to Groh et al. (2013b), Beasor et al. (2020) found that the mass loss rate of RSGs in clusters in the $20-25\,M_\odot$ range was not sufficient to evolve the star to an LBV. Furthermore, the stellar evolution models of Maeder & Meynet (2008) could not explode a star while in the LBV phase. Dwarkadas (2011) argues that stellar models require the outer H-rich envelope of the LBV to be expelled (thus becoming a WR star) before a SN explosion can occur. They suggest that the dense CSM may have been formed over time and the LBV had evolved into a WR star before explosion. However, Groh et al. (2013a) found that if a rotational component was added to stellar evolution models, one could explode a LBV as a SN.

Another possible progenitor of SNe IIn are yellow hyper-giants (YHG), which are post-RSG stars with $M_{ZAMS} \approx 20-60\,M_\odot$ (de Jager 1998). YHGs undergo the considerable mass loss required to form enough CSM for the SN IIn phenomenon and Brennan et al. (2021a,b) found that the SN IIn candidate AT 2016jbu may have a YHG progenitor based on archival data.

1.2.2 *Intermediate mass progenitors*

Some SNe IIn may have lower mass progenitors and alternative explosion mechanisms to the core-collapse scenario.

RSGs are the progenitors of "normal" SNe, such as SNe II-Plateau (SNe IIP) that are named as such due to a plateau in their light curve, due to a recombination wave in a massive H-rich envelope. RSGs suffer mass loss through massive winds and can lose a lot of their H-rich envelope, which may result in a SN II-Linear (SN IIL, named for the linear light curve decay). However, some SNe IIn may have RSG progenitors. Smith et al. (2009) present a study on the galactic RSGs, Betelgeuse and VY CMa. Those authors found that while Betelgeuse had steady mass loss via winds, VY CMa suffered more episodic mass loss. Smith et al. conclude that when considering the density of the CSM surrounding VY CMa, this RSG could be the progenitor for a SN 1988Z-like SN IIn. Another SN IIn with a possible RSG progenitor is SN 1998S where the CSM was produced by a strong wind and also is very dusty (Meikle et al. 2003; Mauerhan & Smith 2012; Taddia et al. 2015).

Electron-capture SNe (ecSNe) arise when a star at the very lowest mass range for CCSNe ($8-10\,M_\odot$) explodes via collapse of its ONeMg degenerate core, resulting from electron capture by ^{24}Mg and ^{20}Ne. Compared to typical SNe II explosions, ecSNe are not as energetic (Miyaji et al. 1980; Nomoto 1984, 1987). Prior to explosion, the progenitors of ecSNe are super-AGB (sAGB) stars and have a CSM cocoon formed from massive winds that creates the SN IIn spectral features. There may be an example of a Galactic ecSN in SN 1054 when one considers the remnant, the Crab Nebula (M 1 Mayall & Oort 1942; Duyvendak 1942; Smith et al. 2013; Moriya et al. 2014). Another clue that ecSNe may produce SNe IIn is that contemporary reports of SN 1054 are not consistent with the lower luminoisity expected from ecSNe. Moriya et al. (2014) investigated whether this higher 'historical' luminosity may be explained with CSM interaction.

Alternative to the core-collapse scenario, a SN Ia exploding in a dense CSM could produce spectral features similar to that of a SN IIn (Deng et al. 2004; Dilday et al. 2012; Silverman et al. 2013).

Hamuy et al. (2003) found that SN 2002ic was the first unambiguous SN Ia-CSM and showed the classic complex, multi-component H Balmer profiles we expect in SNe IIn. A number of SNe IIn have been identified as SNe Ia-CSM at later times when the characteristic SN Ia features become apparent such as broad Si II absorption. Examples include SN 1997cy (Germany et al. 2000; Prieto et al. 2005) and SN 2005gj (Prieto et al. 2005; Aldering et al.

2006). The classification of SNe Ia-CSM can be challenging as the identifying SN Ia features may become apparent at later times. The recent findings of Jerkstrand et al. (2020) suggest the well studied superluminous SN IIn, SN 2006gy may be thermonuclear in origin. Jerkstrand et al. note that the neutral Fe lines seen in the spectra of SN 2006gy at late times (+394 days) were consistent with their SN Ia models where the SN ejecta hit dense CSM.

1.2.3 Supernova Impostors

SN impostors are a part of a more general group known as gap transients that inhabit the gaps in the timescale-luminosity phase space between classical novae and SNe (Kasliwal et al. 2012). SN impostors are typically subluminous compared to 'true' SNe but are more luminous than novae, with impostors having absolute magnitudes $M_V \approx -11$ to -14 (Kochanek et al. 2012). These SN impostors may be the great outbursts of LBVs, similar to the great eruption of η Car (Smith et al. 2011). The progenitor may subsequently be obscured by dust produced after the eruption (Kochanek et al. 2012), however, this is not the case for all impostors, such as SN 2002kg (Kochanek et al. 2012; Humphreys et al. 2014, 2017).

It is possible that SN impostors can precede a 'true' SN such as SN 2009ip in NGC 7259 (Foley et al. 2011; Mauerhan et al. 2013; Pastorello et al. 2013) and SN 2015bh (Boian & Groh 2018; Thöne et al. 2017). However, in the case of SN 2009ip, where there were two outbursts, in 2009 and 2012. Pastorello et al. (2013) and Smith et al. (2014) found that the 2012 eruption was consistent with a terminal CCSN explosion, taking into consideration the high luminosity, explosion energy and the enduring emission features. Fraser et al. (2013), however, reported that the spectra in 2012 were similar to the 2009 eruption, the luminosity had not dropped below pre-discovery levels and there was a lack of expected nucleosynthesised elements.

A noteworthy transient that is the prototype for its own subclass is SN 2008S in NGC 6964 (Arbour 2008; Thompson et al. 2009). The progenitor could not be recovered in optical pre-explosion imaging and Prieto et al. (2008) suggest the progenitor may have a mass of $\sim 10\,M_\odot$ and inhabited a dust-rich environment that shrouded progenitor and thus the transient was an impostor. However, Botticella et al. (2009) reported that the light-curve for SN 2008S was consistent with being powered by ^{56}Co decay and that the progenitor may have been an AGB star and the explosion was a terminal ecSN. Adams et al. (2016) found that SN 2008S had faded, by 2015 to a level dimmer than its progenitor, which may suggest the explosion was terminal, or extreme dust behaviour must be invoked. Another example of a SN impostor is SNhunt248 that had an optical peak magnitude of -15 and appeared to be a YHG with ejecta from the eruption interacting with CSM (Kankare et al. 2015).

1.3 Environmental studies

The local environment of a SN within its host galaxy can offer information on the possible progenitor system. For example, one can examine the association of SNe to ongoing star-formation as traced by Hα emission. Generally speaking, SNe II trace regions of recent star formation and the most massive stars may trace ongoing star formation (see, for example Anderson & James 2009; Habergham et al. 2014). Hα emission indicates a characteristic time-scale of under 16 Myr (Haydon et al. 2020). Possible high mass and short lived progenitors, such as LBVs, would be expected to be found in regions of ongoing star formation, which would be traced by Hα emission.

Another way the environments of SNe have been probed is through the radial distributions of SNe in terms of the observed flux in a particular filter (we describe this method in Section 2.4). Habergham et al. (2014) found that the radial distribution of SNe IIn in their sample were very different from the radial distributions of SNe Ic. The SNe Ic were centrally located (hence a higher metallicity region) and they did not find a central concentration of SNe IIn. This suggests the two classes arise from different stellar populations.

Habergham et al. (2014) use the O3N2 diagnostic (Pettini & Pagel 2004) to compare the metallicity at the sites of different SN classes. It was found that SN IIn environments are more metal rich than SNe IIP and that the local metallicities of SN impostors tend to be lower than SNe Ic, IIn or IIP. Taddia et al. (2015) use optical spectra of 60 interacting transients (SNe IIn, SNe Ibn and impostors). Taddia et al. found that impostors were generally in regions of lower metallicity when compared to SNe IIn. SNe IIn similar to SN 1998S were found in higher metallicity regions than SNe IIL and SNe IIP, and long lasting SNe IIn, such as SN 2005ip and SN 1988Z, were in regions of lower metallicity as seen in the environments of SN impostors. Habergham et al. conclude that SN IIn environment variation suggests there may be multiple progenitor paths rather than solely LBVs.

1.4 This paper

In this paper, we use a vastly expanded SN IIn sample to probe the possible progenitor paths using local host galaxy information . Using pixel statistics techniques and observations from our Hα SNe IIn host survey, we present the largest environmental study of SNe IIn to date. We outline our SN IIn sample selection, observations and data analysis in Section 2. In Section 3 we present our target catalogue and results of our host galaxy analysis along with example images of the hosts. We then discuss our results and their implications for the progenitor channels of SNe IIn in Section 4.

2 METHODS

2.1 The classification of type IIn supernovae and our sample

Perhaps due to the diversity of SNe IIn, classification can be difficult. One may group SNe IIn into groups of similar objects, for example, SN 1988Z-like which have slow photometric evolution, SN 1994W-like with a plateau in the light curve lasting a few months preceding a rapid decline, and SN 1998S-like that have a fast rise and decline time in the light-curve. Ransome et al. (2021, hereafter RHD21) introduced a classification scheme for SNe IIn, mostly based on the complex, multi-component Hα profiles. In this scheme, transients are split into three groups, gold, silver, and not SNe IIn. Gold SNe IIn exhibit enduring CSM interaction features, silver SNe IIn show weaker CSM interaction or have a single spectrum available. RHD21 found that 28 of SNe of the 87 in their sample of SNe, may have previously been misclassified. RHD21 produced a robust, systematically classified sample of SNe IIn which we use in our environmental analysis.

Our sample is outlined in Table 1. The table contains the SNe, RHD21 spectral category and the telescope used. Most of our observations are in the Northern hemisphere, however, three of our SNe IIn observed with LCOGT 2m located in Australia.

2.2 Observations

In the Northern Hemisphere, we utilised the Liverpool Telescope (LT; Steele et al. 2009) and Isaac Newton Telescope (INT) at the Observatorio de Roque de las Muchachos on La Palma in the Canary Islands. For our observations on the LT, we use the IO:O instrument[1]. We use the Wide Field Camera (WFC) on the INT[2]. In the Southern Hemisphere, we use the Las Cumbres Observatory 2m (LCOGT 2m) at Siding Springs Observatory, New South Wales, Australia (Brown et al. 2013). We use Spectral[3] on the LCOGT 2m.

Our observations consist of 3×300 s exposures using the appropriate redshifted Hα filter and a single 300 s exposure with in the r'-band with 2×2 binning. These observations span 2019 to 2021. We limit our observations to nearby ($z < 0.02$) hosts as we require that H II regions are resolved for the pixel statistics described in Section 2.3. Furthermore, we select hosts with axial ratios of under 4:1 to ensure the SN IIn site is associated with the observed emission, rather than possibly coincident as may be the case in a more edge-on galaxy. Major and minor axes for each host were taken from the SIMBAD Astronomical Database (Wenger et al. 2000). Both IO:O and Spectral have a 10′ field of view and all surveyed hosts were contained within the field of view. The LT has redshifted Hα filters covering the range to around $z = 0.04$ and all of our targets are within $z = 0.02$. We only use the LCOGT 2m for nearby targets as there is only a rest-frame Hα filter.

Raw data from the LT and LCOGT 2m are reduced by the respective standard pipelines (Barnsley et al. 2016; Brown et al. 2013). The NCR analysis requires continuum-subtracted images. We use the methods in Anderson et al. (2012) but using IRAF (Tody 1986), astropy (The Astropy Collaboration et al. 2013) and specutils (Earl et al. 2022). Data from the INT was reduced using standard procedures using astropy.

2.3 Pixel statistics: normalised cumulative ranking

NCR was first implemented by James & Anderson (2006) and subsequently utilised in environmental studies (e.g., Anderson & James 2008; Anderson et al. 2012; Habergham et al. 2014). NCR traces the association of a pixel with some emission, in our case, to Hα emission and therefore, the association to ongoing star-formation. NCR assigns every pixel a value between zero and one. NCR is calculated by ordering the the pixel values of the continuum-subtracted Hα image in ascending order, summing these values and normalising by the sum. A zero NCR value indicates no Hα emission and therefore no association with ongoing star-formation. An NCR value of one indicates the strongest star-forming pixel within the entire galaxy image. After continuum subtraction, some pixels will have negative values. Pixels before the sum turns positive are assigned an NCR value of zero. The NCR value of a pixel may be written as,

$$\mathrm{NCR_i} = \frac{\sum_1^i x_i}{\sum_1^N x_N},$$

where i is the current pixel, N is the total number of pixels and x is the pixel value.

Using NCR analysis, Anderson & James (2008) found that SNe IIn in their sample did not follow the Hα emission in their hosts. Those authors did, however, note that the SNe IIn more closely followed near-ultraviolet (NUV) emission when comparing data from the *Galaxy Evolution Explorer* (GALEX, Martin et al. 2003). NUV traces recent star-formation with a characteristic time-scale of over around 19.6 Myr for *GALEX* NUV (Haydon et al. 2020).

Anderson et al. (2012) set out to constrain progenitor properties using the SN association to Hα and NUV emission. They found that there was a mass ladder in terms of association to Hα emission with the most massive progenitors being most associated with ongoing star formation, owing to their shorter lifetimes. It was found that the mass sequence, starting with SNe Ic (see also, Kangas et al. 2013) as the most massive and most associated, went as such:

SNe Ic $\rightarrow$ SNe Ib $\rightarrow$ SNe II $\rightarrow$ SNe Ia.

Anderson et al. suggested that this indicated that the majority of SNe IIn do not have high-mass progenitors, such as LBVs. However, Smith & Tombleson (2014) noted that LBVs are often not associated with clusters of O-stars as one would expect of a massive progenitor. Instead those authors suggest that many LBVs may form in binary systems where the LBV is a mass gainer and a WR star is a donor in situ in the home O-star cluster.

Habergham et al. (2014) investigated the environments of SNe IIn and SN impostors. There were 24 SNe IIn in their sample and again it was found that these transients did not follow star formation as traced by Hα, via the NCR method. Habergham et al. conclude that as some SNe IIn do have LBV progenitors, there may be multiple progenitor channels for SNe IIn.

Additionally, Kangas et al. (2017) utilised the NCR method with resolved massive stars in the Large Magellanic Cloud (LMC) and M33. Kangas et al. compare the NCR distributions of the massive stars in their sample with the NCR distributions of the different classes of SNe in Anderson et al. (2012). Kangas et al. note that SNe IIn are a diverse class, possibly with multiple progenitors. Those authors suggest that when combining the NCR values of RSGs ($M \lesssim 8\,M_\odot$) and LBVs (with RSGs making up 70% and LBVs accounting for 30% of the NCR values), the average SN IIn NCR value can be reproduced.

To compute the NCR value, the average NCR value of a 3×3 pixel bin centred around the target pixel is taken. We apply this to our sample and then make cumulative distributions. We split our sample into the spectral categories in RHD21 and then compare these distributions to each other and also a hypothetical 1:1 relation which represents an NCR distribution that 'perfectly' follows the emission.

We can then implement Anderson-Darling (AD, Anderson & Darling 1952; Stephens 1974) and Hartigan dip tests (HDT Hartigan & Hartigan 1985), as well as the bimodality coefficient (Institute 1989) in order to test whether there may be multiple populations of SNe IIn in terms of their association to ongoing star-formation as traced by Hα emission.

2.4 Radial analysis

The radial distribution of SNe can indicate the general stellar population. In spiral galaxies, the bulge tends to have an older population while the discs have younger populations with active star formation. Furthermore, the spatial distribution within a galaxy may provide an analogue for metallicity as there is a metallicity gradient (Henry & Worthey 1999) with central regions having a higher metallicity than further out in the disc regions.

[1] https://telescope.livjm.ac.uk/TelInst/Inst/IOO/
[2] https://www.ing.iac.es//Astronomy/instruments/wfc/
[3] https://lco.global/observatory/instruments/spectral/

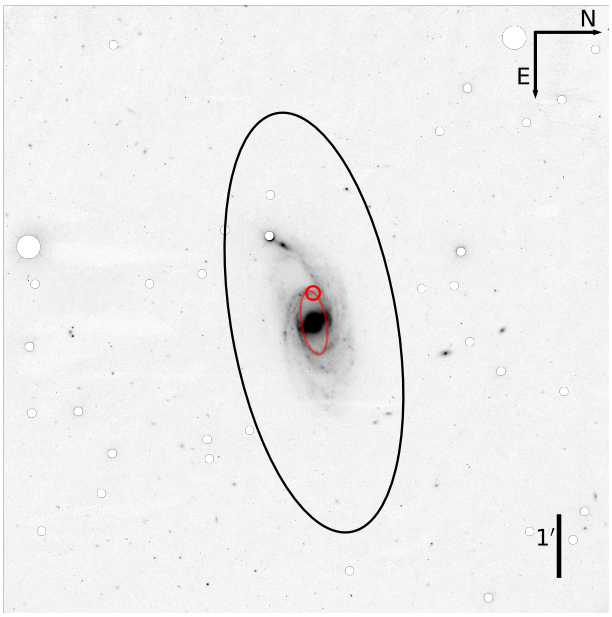

Figure 1. An example of the radial analysis employed in this paper. Shown is the r'-band image of the host of PTF 11iqb, NGC 151 (z=0.0126). The red ellipse just intercepts the SN IIn site (red circle). The black ellipse encloses the galaxy r'-band flux. These ellipses are also used in the continuum subtracted Hα image. In order to measure the emission from the host, foreground stars were masked.

We measure and compare the radial distribution of our SNe IIn in terms of the r'-band and Hα flux in their host galaxies. We adopt the method used in Anderson & James (2009). This is achieved calculating the ratio of ellipses that cover the extent of the host r'-band light and the ellipse enclosing the SN position. Ellipse parameters were taken from the NASA/IPAC Extragalactic Database (NED Helou & Madore 1988). For the ellipse covering the total r'-band emission from the host, the semi-major axis is increased until the ellipse has reached the sky level on the r'-band image. The sky level of the image is determined such that the difference in enclosed flux between ellipses has flattened out to being around zero. This ellipse is then used with the continuum subtracted Hα image. This gives us Fr(R), the fraction of r'-band light contained within the SN ellipse and Fr(Hα), the fraction of Hα emission contained in the SN ellipse. Therefore each SN will have a Fr(R) and an Fr(Hα) value of between 0 and 1, where 0 indicates the SN is at the centre of the host and a value of 1 indicates the SN is at the extreme periphery of the host. For this radial analysis, it is important to mask stars such that the measured flux is from the host. Using the results from the `starfind` and `xyxymatch` subroutines in IRAF, the (non-saturated) stars are detected and masked. Saturated stars are not detected by `starfind` so these are masked by eye. This is carried over to the continuum subtracted Hα images to eliminate artefacts that can be left over after continuum subtraction. In Fig. 1 we present an example of this radial analysis, where we show the ellipse enclosing the full r'-band flux of the host galaxy and the ellipse that just encloses the SN pixel.

Using these statistical measures, we will now analyse the SN IIn populations in host galaxies within z = 0.02.

3 RESULTS

3.1 The hosts

Our observing campaign spanning from July 2019 – July 2021 increased the sample size of SN IIn hosts (within z < 0.02) from previous studies (24) to 78. Of these, we observe 30 gold and 34 silver SNe IIn classified by RHD21. The remaining observations were hosts of SN IIn without any public spectral data so were not spectrally reclassified but are classified as SNe IIn on public databases.

In Fig. 2 – Fig. 3 we present the two of our SNe IIn shown in both the r'-band and continuum subtracted Hα images. We also mark the SN positions with a red circle. We present the full sample of SNe IIn we have host observations for in Table 1.

In Table 1 we present our full sample of 77 SNe IIn with their NCR values, classification from RHD21, Fr(Hα) values, Fr(R) values, and the telescope used in the observations. Most of our observations were from the Northern Hemisphere, however three of our SNe IIn are southern targets observed with LCOGT 2m. The Southern Hemisphere sub-sample is somewhat small due to the limited Hα filters available at LCOGT 2m.

3.2 NCR analysis results

We show the results of our NCR analysis in Fig. 4. We compare sub-samples of SN IIn NCR values to a 1:1 NCR value relationship, which represents a hypothetical population of transients that perfectly traces Hα emission (and therefore, ongoing star formation). The full sample has a mean NCR value of 0.306 ± 0.041 and the non-zero NCR subsample has a mean of 0.521 ± 0.038. A mean NCR value of around 0.500 would suggest a population that follows the emission.

In Table 2 we present the AD p-values of different sub-samples of our NCR values when compared to each other and to a hypothetical population that perfectly follows Hα emission. An AD test p-value ≤ 0.05 suggests that two populations differ significantly and are likely to be drawn from separate parent populations. We find that our full sample (blue line in Fig. 4) of SNe IIn does not follow star-formation as traced by Hα emission when compared with the hypothetical population that traces star-formation perfectly, with an AD p-value $\sim 10^{-6}$. We then split our full sample into the gold and silver spectral subcategories from RHD21 and again these sub-samples likely do not follow the Hα emission and are similar to each other and the full sample. However, when we split the sample and isolate the non-zero NCR SNe IIn we find that the AD p-value (0.37) is consistent with the non-zero NCR sub-sample being drawn from the same population as the perfectly 1:1 relation. Therefore, the non-zero NCR SN IIn sub-sample is likely to follow the Hα emission and therefore appears correlated with (on-going) star formation.

The statistics so far suggest that we are observing multiple populations within the SN IIn class when considering NCR distributions. In order to test for multi-modality, we utilise HDT and the bimodality co-efficient. A HDT p-value ≤ 0.05 indicates the sample is significantly multi-modal and a HDT p-value of $0.05-0.10$ suggests multi-modality of marginal significance. The bimodality coefficient uses the skew and kurtosis of a distribution and bimodality coefficient of $> 5/9$ suggests a bimodal distribution.

We have applied these tests to our sub-samples with the results presented in Table 3. The HDT p-values indicate that the full sample is at least bimodal with HDT p-values in the order $\sim 10^{-3}$. However and non-zero NCR sub-samples do not show significant levels of bimodality according to the HDT. None of our sub-samples have a bimodality coefficient $> 5/9$, which suggests our NCR values do

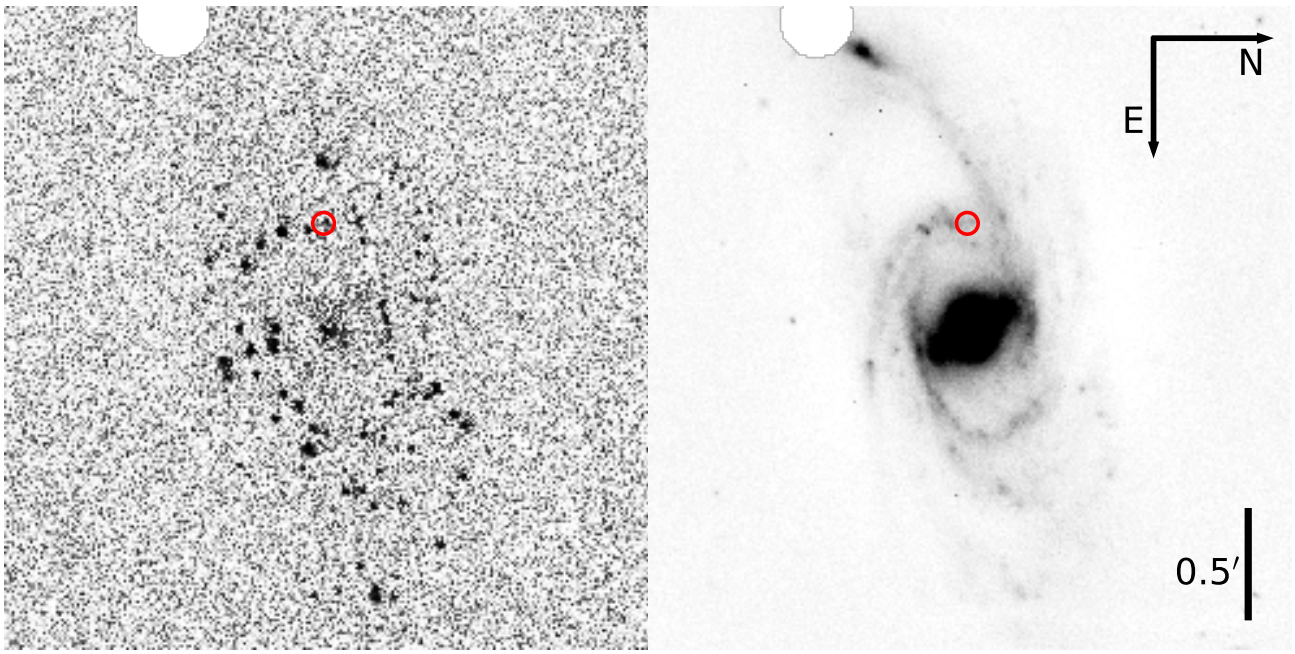

Figure 2. The continuum-subtracted Hα (*left*) and r'-band (*right*) environments of PTF 11iqb in NGC 151 (z=0.0126). The position of PTF 11iqb is marked with the red circle. PTF 11iqb is an example of a SN IIn associated with star-formation as traced by the Hα emission, resulting in an NCR value of 0.845. The foreground star at the top of the image has been masked out in the Hα image as the continuum subtraction leaves artefacts which may interfere with the NCR value calculation.

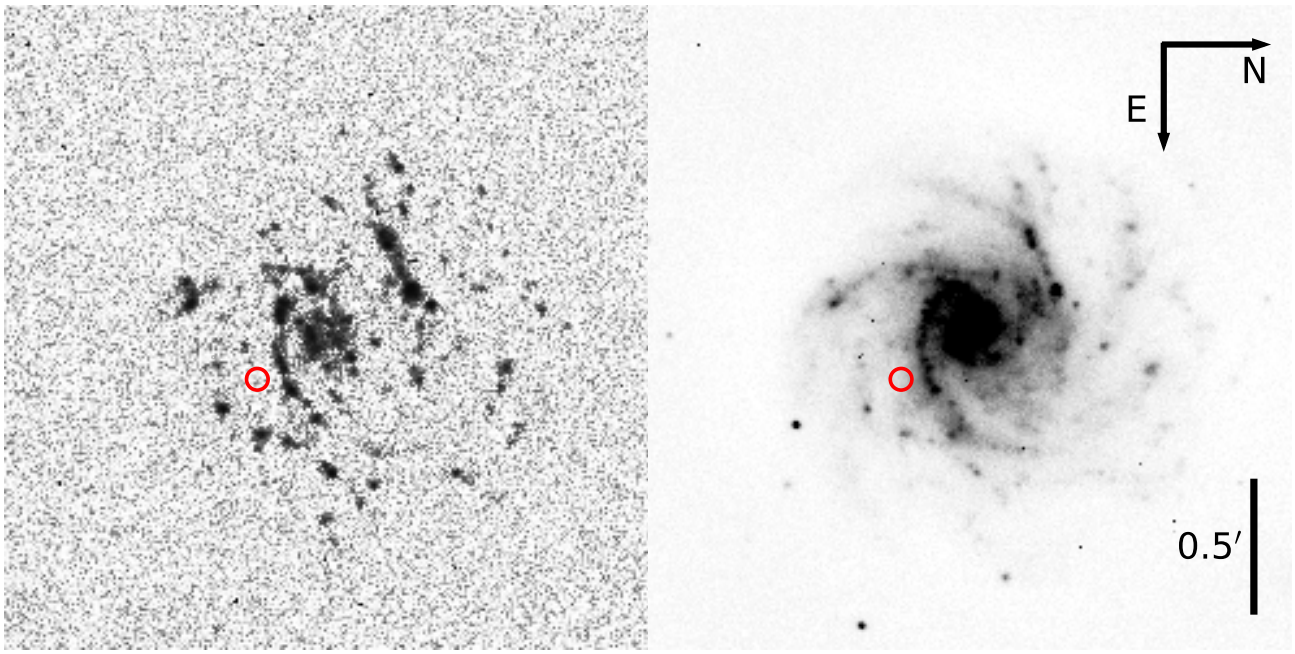

Figure 3. The continuum-subtracted Hα (*left*) and r'-band (*right*) environments of SN 2003lo in NGC 1376 (z=0.0139). The position of SN 2003lo is marked with the red circle. SN 2003lo is an example of a SN IIn that is not associated with star-formation as traced by the Hα emission (NCR value of zero). In the case of SN 2003lo, the transient resides in an apparent inter-arm gap.

Table 1. Our sample of 77 SNe IIn and their hosts with the discovery date, coordinates, NCR value, Fr(Hα) values, Fr(R) value, the telescope we used for the observation and the classification from RHD21.

Name	Disc. Date	Host	R.A.	Dec.	z	Telescope	NCR value	Classification	Fr(Hα)	Fr(R)
SN 2005db	2005/07/19	NGC 214	00:41:26.79	25:29:51.60	0.0151	LT	0.387	Gold	0.528	0.526
SN 2005gl	2005/10/05	NGC 266	00:49:50.02	32:16:56.80	0.0155	LT	0.765	Gold	0.644	0.526
SN 1999eb	1999/10/02	NGC 664	01:43:45.45	04:13:25.90	0.0180	LT	0.750	Gold	0.324	0.258
SN 2003G	2003/08/01	IC 208	02:08:28.13	06:23:51.90	0.0120	LT	0.000	Gold	-	-
SN 2008J	2008/01/15	MCG -02-07-33	02:34:24.20	-10:50:38.50	0.0159	LT	0.808	Gold	0.069	0.077
SN 2000eo	2000/11/16	MCG -02-09-03	03:09:08.17	-10:17:55.3	0.0100	LT	0.000	Gold	-	-
SN 2006gy	2006/09/18	NGC 1260	03:17:27.06	41:24:19.5	0.0192	LT	0.907	Gold	0.014	0.030
SN 1989R	1989/10/14	UGC 2912	03:59:32.56	42:37:09.20	0.0180	LT	0.199	Gold	-	-
SN 1995G	1995/02/23	NGC 1643	04:43:44.26	-05:18:53.70	0.0160	LT	0.007	Gold	0.549	0.620
SN 2006jd	2006/10/12	UGC 4179	08:02:07.43	00:48:31.50	0.0186	LT	0.879	Gold	0.411	0.580
SN 2009kn	2009/10/26	MCG -03-21-06	08:09:43.04	-17:44:51.30	0.0143	LT	0.000	Gold	-	-
SN 2005kj	2005/11/17	A084009-0536	08:40:09.18	-05:36:02.20	0.0160	LT	0.000	Gold	-	-
SN 1994ak	1994/12/24	NGC 2782	09:14:01.47	40:06:21.50	0.0085	LT	0.000	Gold	0.955	0.869
SN 2005ip	2005/11/05	NGC 2906	09:32:06.42	08:26:44.40	0.00718	LT	-	Gold	0.685	0.540
SN 1989C	1989/02/03	MCG +01-25-25	09:47:45.49	02:37:36.10	0.0063	LT	0.830	Gold	-	-
SN 2011ht	2011/09/29	UGC 5460	10:08:10.56	51:50:57.12	0.0036	LT	0.000	Gold	0.090	0.197
SN 1993N	1993/04/15	UGC 5695	10:29:46.33	13:01:14.00	0.0098	LT	0.000	Gold	0.485	0.490
SN 1998S	1998/03/02	NGC 3877	11:46:06.13	47:28:55.40	0.0030	LT	0.780	Gold	-	-
SN 1994W	1994/07/29	NGC 4041	12:02:10.92	62:08:32.70	0.0040	LT	0.000	Gold	0.698	0.510
SN 2011A	2001/01/02	NGC 4902	13:01:01.19	-14:31:34.80	0.0089	LT	0.000	Gold	0.385	0.607
SN 2016bdu	2016/02/28	-	13:10:13.95	32:31:14.07	0.0170	LT	0.707	Gold	-	-
SN 1997eg	1997/12/04	NGC 5012	13:11:36.73	22:55:29.40	0.0087	LT	0.784	Gold	0.454	0.523
SN 2015da	2015/01/09	NGC 5337	13:52:24.11	39:41:28.60	0.0072	LT	-	Gold	0.447	0.564
SN 1994Y	1994/08/19	NGC 5371	13:55:36.90	40:27:53.40	0.0085	LT	0.000	Gold	0.112	0.320
SN 1995N	1995/05/05	MCG-02-38-17	14:49:28.29	-10:10:14.40	0.0062	LT	0.000	Gold	-	-
SN 2008B	2008/01/02	NGC 5829	15:02:43.65	23:20:07.80	0.0188	LT	0.000	Gold	0.201	0.383
SN 1987B	1987/02/24	NGC 5850	15:07:02.92	01:30:13.20	0.0085	LT	0.107	Gold	0.998	0.999
SN 2008S	2008/02/01	NGC 6946	20:34:45.35	60:05:57.80	0.0002	LT	0.000	Gold	-	-
SN 1999el	1999/10/20	NGC 6951	20:37:18.03	66:06:11.90	0.0047	INT	0.000	Gold	0.277	0.321
SN 2009ip	2012/07/14	NGC 7259	22:23:08.30	-28:56:52.40	0.0059	LCOGT 2m	0.000	Gold	0.788	0.891
SN 2019el	2019/01/02	-	00:02:56.70	+32:32:52.30	0.0005	LT	0.003	Silver	-	-
SN 2017hcc	2017/10/02	GALEX 2.67E+18	00:03:50.58	-11:28:28.78	0.0173	LT	0.993	Silver	-	-
SN 2011fx	2011/08/30	MCG+04-01-48	00:17:59.56	24:33:46.00	0.0193	LT	0.726	Silver	-	-
PTF 11iqb	2011/07/23	NGC 151	00:34:04.84	-09:42:17.90	0.0125	LT	0.845	Silver	0.059	0.334
SN 2007pk	2007/11/10	NGC 579	01:31:47.07	33:36:54.10	0.0167	LT	0.785	Silver	0.248	0.108
SN 2016eem	2016/07/08	-	02:05:59.80	47:44:14.00	0.0200	LT	0.231	Silver	-	-
SN 2002ea	2002/07/21	NGC 820	02:08:25.08	14:20:52.80	0.0148	LT	0.096	Silver	0.124	0.308
SN 1978K	1978/07/31	NGC 1313	03:17:38.60	-66:33:04.60	0.0016	LCOGT 2m	0.705	Silver	-	-
SN 2003lo	2003/12/31	NGC 1376	03:37:05.12	-05:02:17.30	0.0140	LT	0.000	Silver	0.288	0.391
SN 2005aq	2005/03/07	NGC 1599	04:31:38.79	-04:35:06.80	0.0130	LT	0.370	Silver	0.399	0.291
Gaia14ahl	2014/09/20	PGC 1681539	04:42:12.09	23:06:15.00	0.0170	LT	0.000	Silver	-	-
SN 2005ma	2005/12/24	MCG -02-13-13	04:49:53.91	-10:45:23.40	0.0150	LT	0.262	Silver	0.374	0.373
SN 2016hgf	2016/10/16	WEIN 69	04:51:45.97	44:36:03.06	0.0172	LT	0.000	Silver	0.280	0.217
SN 2019rz	2019/01/14	UGC 3554	06:50:25.80	43:03:11.70	0.0189	LT	0.926	Silver	0.028	0.001
AT 2018lkg	2018/12/30	UGC 3660	07:06:34.76	63:50:56.90	0.0142	LT	0.880	Silver	0.092	0.001
AT 2014eu	2014/11/17	MCG+09-13-02	07:28:55.97	56:11:46.20	0.0179	LT	0.228	Silver	-	-
SN 2014ee	2014/11/12	UGC 4132	07:59:11.68	32:54:39.60	0.0174	LT	0.590	Silver	0.796	0.655
SN 2002fj	2002/09/12	NGC 2642	08:40:45.10	-04:07:38.50	0.0140	LT	0.414	Silver	0.268	0.348
SN 2015bh	2015/02/07	NGC 2770	09:09:34.96	33:07:20.40	0.0064	LT	0.000	Silver	0.601	0.603
SN 2014es	2014/11/20	MCG -01-24-12	09:20:46.91	-08:03:34.00	0.0196	LT	0.000	Silver	0.900	0.876
SN 1997ab	1997/02/28	A095100+2004	09:51:00.40	20:04:24.00	0.0130	LT	0.000	Silver	-	-
SN 1996bu	1996/1/14	NGC 3631	11:20:59.18	53:12:08.00	0.0039	LT	0.026	Silver	-	-
SN 1987F	1987/03/22	NGC 4615	12:41:38.99	26:04:22.40	0.0160	LT	0.000	Silver	0.132	0.152
SN 2008ip	2008/12/31	NGC 4846	12:57:50.20	36:22:33.5	0.0151	LT	0.000	Silver	0.227	0.902
SN 2006am	2006/02/22	NGC 5630	14:27:37.24	41:15:35.40	0.0089	LT	0.555	Silver	0.894	0.683
SN 2003dv	2003/04/22	UGC 9638	14:58:04.92	58:52:49.90	0.0076	LT	0.180	Silver	1.000	0.777
SN 2016bly	2016/04/29	2MASX J17224883+1400584	17:22:48.90	14:00:59.88	0.0194	LT	0.840	Silver	-	-
SN 2017gas	2017/08/10	2MASX J20171114+5812094	20:17:11.32	58:12:08.00	0.0100	LT	0.920	Silver	-	-
SN 2006bo	2006/04/05	UGC 11578	20:30:41.90	09:11:40.80	0.0153	LT	0.000	Silver	-	-
SN 2018hpb	2018/10/25	-	22:01:34.52	-17:27:45.22	0.0177	LT	0.000	Silver	-	-
SN 2013fs	2013/10/07	NGC 7610	23:19:44.70	10:11:05.00	0.0119	LT	0.345	Silver	0.515	0.660
SN 2015bf	2015/12/12	NGC 7653	23:24:49.03	15:16:52.00	0.0142	LT	0.657	Silver	0.349	0.630
SN 2010jj	2010/11/03	NGC 812	02:06:52.23	44:34:17.50	0.0172	LT	0.000	-	0.103	0.179
PS 15cwt	2015/08/20	-	02:33:16.24	19:15:25.20	0.0135	LT	0.012	-	-	-
SN 2011js	2011/12/31	NGC 1103	02:48:04.96	-13:57:51.10	0.0138	LT	0.000	-	0.262	0.385
SN 2006qt	2006/10/11	A034002-0434	03:40:02.72	-04:34:18.70	0.0100	LT	0.000	-	-	-
SN 2005kd	2005/11/12	PGC 14370	04:03:16.88	71:43:18.90	0.0150	LT	0.000	-	-	-
SN 2007ak	2007/03/10	UGC 3293	05:20:40.75	08:48:16.00	0.0156	LT	0.000	-	0.184	0.130
SN 2013ha	2013/11/06	MCG +11-08-25	06:15:49.85	66:50:19.40	0.0131	LT	0.808	-	-	-
SN 1987C	1987/03/21	MCG+09-14-47	08:30:01.30	52:41:33.00	0.0142	LT	0.146	-	0.632	0.926
SN 2016ehw	2016/07/20	MCG+12-08-47	08:36:37.60	73:35:03.70	0.0120	LT	0.041	-	-	-
ASASSN-15lf	2015/06/15	NGC 4108	12:06:45.56	67:09:24.00	0.0084	LT	0.000	-	0.638	0.645
SN 2012ab	2012/01/31	A122248+0536	12:22:47.60	05:36:25.00	0.0180	LT	0.912	-	-	-
PS 15aip	2015/05/02	KUG 1319+356	13:21:55.23	35:21:32.00	0.0195	LT	0.860	-	-	-
SN 2006M	2006/01/17	PGC 47137	13:27:19.76	31:47:14.50	0.0150	LT	0.575	-	-	-
SN 1978G	1978/11/24	IC 5201	22:20:48.30	-46:01:22.00	0.0031	LCOGT 2m	0.000	-	-	-
SN 2006dn	2006/07/05	UGC 12188	22:47:37.84	39:52:50.16	0.0171	LT	0.434	-	0.059	0.053

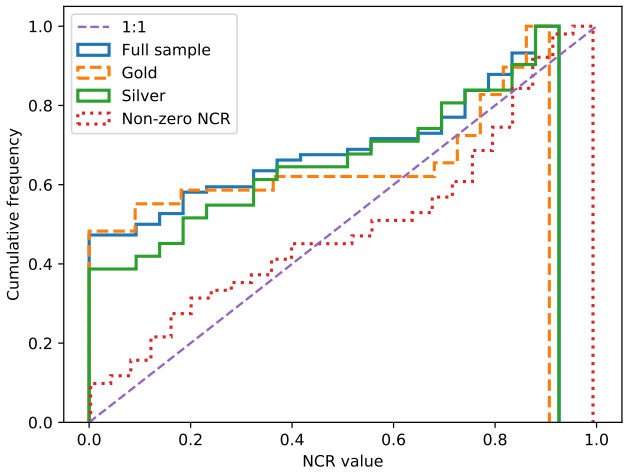

Figure 4. Cumulative distribution of the NCR values of the subsamples of our SNe IIn environments. The solid blue line is the full sample, the orange dashed line is the gold sample, the solid green line is the silver sample and the red dashed line is the non-zero NCR value sample. Also plotted is the 1:1 relationship (purple dashed line) which represents a population of progenitors which are strongly associated with star formation as traced by Hα emission.

not show bimodality. However this does not rule out multi-modality as suggested by the HDT p-values for the full sample.

3.3 Radial analysis results

We present histograms showing the distributions of the fraction of r'-band or Hα flux contained within the ellipse that just intersects the SN pixel. Fig. 5 shows the histogram for the distribution of the Hα fraction, Fr(Hα), and r'-band faction, Fr(R).

The sample of 45 SN IIn hosts used in the radial analysis is smaller than the full sample as this analysis requires hosts that are well defined such that a radial profile can be constructed. This will rule out hosts with semi-major axes of under ~ 0.5'. The mean Fr(R) value is 0.454 ± 0.040 and the mean Fr(Hα) values is 0.413 ± 0.042. From the histograms in Fig. 5 we can see that there may be a hint of a peak at lower Fr(Hα) values which indicates centrally concentrated SNe but generally, the radial Hα distribution is fairly evenly distributed. The Fr(R) distribution tells a similar story, the radial distribution is fairly evenly distributed. More data is needed in order to determine any possible trends here. This is consistent with the findings of Habergham et al. (2014).

In Table 3 we show the the HDT p-values and the bimodality coefficients for our Fr(R) and Fr(Hα) value distributions. For both of these distributions, no bimodality was found by either the HDT or the bimodality coefficient.

4 DISCUSSION

We have carried out the largest Hα survey of nearby ($z < 0.02$) SN IIn hosts, almost quadrupling the sample size from previous studies. The association of the environments of a sample of 77 nearby SNe IIn to Hα emission and therefore ongoing star-formation was measured.

Table 2. The multi-sample Anderson-Darling test results comparing the NCR values of our sub-samples of SNe IIn. These tests probe whether or not the sub-samples are drawn from the same parent population.

Sample	AD p-value
Full sample – 1:1	2.7×10^{-8}
Gold – 1:1	8.5×10^{-5}
Silver – 1:1	1.0×10^{-3}
Non-zero NCR – 1:1	0.37
Gold – Full sample	0.79
Silver – Full sample	0.72
Non-zero NCR – Full sample	3.6×10^{-6}
Gold – Silver	0.27
Gold – Non-zero NCR	7.0×10^{-5}
Silver – Non-zero NCR	4.3×10^{-3}

Table 3. The Hartigan's dip test and bimodality coefficients for our sub-samples of SNe IIn and the flux fractions.

Sample	HDT p-value	Bimodality coefficient
Full sample	7.9×10^{-3}	0.23
Non-zero NCR	4.7×10^{-2}	0.19
Fr(Hα)	0.87	0.32
Fr(R)	0.38	0.26

4.1 Constraining progenitor systems

The relations in the NCR values presented in Section 3 enable inferences to be made on the underlying stellar population. Anderson et al. (2012) investigated the association of a large sample of CCSNe with the host galaxy star formation using the NCR pixel statistics method and found a mass ladder in terms of progenitor mass and NCR value distribution.

Some SNe Ic progenitors are WR stars (Georgy et al. 2009) and LBVs may be a preceding evolutionary stage to WR stars. It is known that at least some SNe IIn have LBV progenitors (e.g, SN 2005gl Gal-Yam et al. 2007). One would therefore expect that SNe IIn would follow ongoing star-formation as traced by Hα emission if the main progenitor path for SNe IIn were LBVs. However, this is not what we observe in our environmental analysis. We found that over 40% of our sample had an NCR value of zero, indicating the SN pixel had **no** association with the Hα emission. When we isolate the non-zero NCR values we find that when we compare the NCR values to a 1:1 relationship, we find that the non-zero NCR values follow this 1:1 distribution. The AD test p-values suggest these two samples are drawn from the same parent population. This may indicate that there are at least two populations of SNe IIn: a non-zero NCR group that follows Hα emission and a population of zero NCR values. This may indicate that these SNe IIn have different progenitor stars. Instead, if we assume that LBVs are the progenitor system of the vast majority of SNe IIn (with the rest being made up of transients such as SNe Ia-CSM or ecSNe) then this may inform us about the evolution and environments of LBVs. Some LBVs may reside in areas outside of a star formation region in their hosts (Smith & Tombleson 2014). Smith & Tombleson found that the neither the Galactic LBVs or LBVs in the LMC and SMC were well associated with O-type star clusters. Further to this, Smith & Tombleson note that in the LMC, the LBVs were more isolated than the Galactic

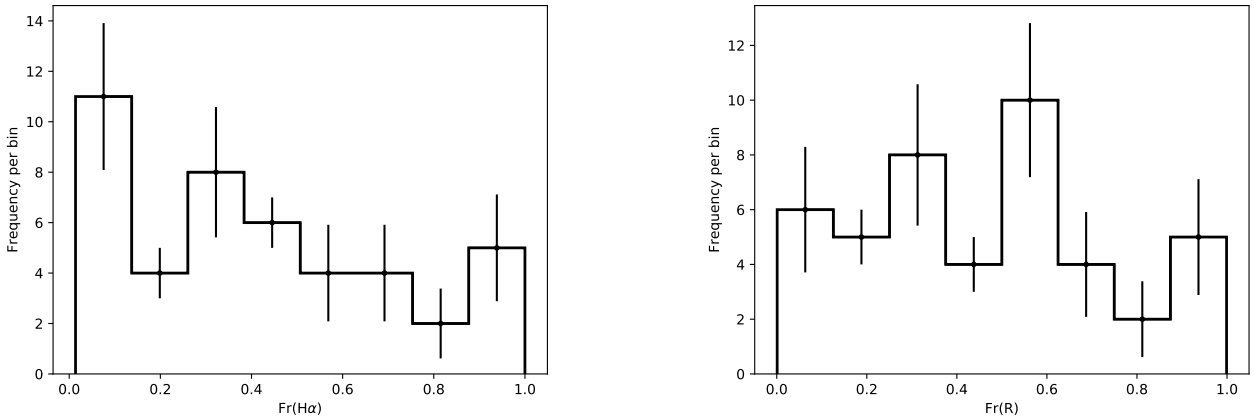

Figure 5. Left: Fraction of Hα, Fr(Hα) flux contained within an ellipse that just encloses the SN pixel. Right: Fraction of r'-band flux contained within the ellipse that just enclosed the SN pixel. The y-axis on these plots is the number of SNe in each bin.

or SMC LBVs and were more isolated than the known WR stars in the LMC. Those authors suggest that LBVs may not be single stars but evolve in binaries (as many O-type stars do, Gies 1987; García & Mermilliod 2001; Evans et al. 2006). Furthermore, LBVs that are isolated and apparently in single star systems may have evolved in a multiple star system and then either the companion star has exploded as a SN or the LBV got kicked out of the system due to interactions with nearby stars and became a "runaway" star. This may cause a spin-up of the LBV, which is consistent with the models of Groh et al. (2013b) where the LBVs in their models exploded as SNe IIn when a rotational element was added. Aghakhanloo et al. (2017) implemented models of LBV isolation and found that observed isolation of some LBVs is consistent with binary evolution. Smith et al. (2020) present a study on the LBV candidate, MCA-1D (also known as UIT003) in the outskirts of M33. Smith et al. find that similarly to some observed SN impostors, MCA-1D had an outburst in 2010 that had a similar light-curve to other LBV outbursts. This LBV candidate is associated with a small cluster but is on the outskirts of the galaxy and the environment is similar to that of the impostor turned (possible) SN IIn, SN 2009ip (see Section 4.3). Humphreys et al. (2016) found that the velocities of seven M31 LBVs and seven M33 LBVs were inconsistent with a runaway star scenario.

Generally, we have found that the progenitors of SNe IIn are longer lived than their host star forming regions which is indicated by the low average NCR values. We also found that the non-zero NCR subsample follows the Hα emission, indicating that the progenitors in the non-zero NCR subsample resided in their star formation regions. Therefore we observe a young population and an older population. These two populations suggest that the SNe IIn do not have a single progenitor path. There is potential degeneracy in the environments of LBVs or LBV-like objects which may contaminate the non-zero NCR sample. Perhaps the contrast we see in environments can not simply be pinned to two sets of separate progenitors, with a higher mass component following ongoing star-formation and another population with lower mass progenitors that are less or unassociated with star formation. This would be consistent with the HDT and bimodality coefficient test results. These open questions prevent a clean distinction between the progenitor environments and masses as LBVs may be isolated and in OB star associations, have an unstable LBV classification or some may even be be formed by lower mass stars merging.

Furthermore, when we split the sample into the gold and silver spectral categories (RHD21), we find that the gold and silver SNe IIn are drawn from the same parent population, as indicated by the AD test p-values. This indicates that the objects in the two categories may similar progenitor types and there is there is unlikely to be a spatial difference between the gold and silver groups. Therefore this indicates that many of the silver SNe IIn may be promoted to a fully fledged gold SN IIn if follow-up observations were taken as suggested by RHD21.

The inference that transients strongly associated with star formation as traced by Hα emission are more likely have very massive progenitors is based upon the assumption that such transients have young, massive progenitors. Hα emission has a characteristic timescale of < 16 Myr (Haydon et al. 2018, 2020) so one would expect that SNe appearing in these regions (correlated with H II regions Kuncarayakti et al. 2013) are young and massive and therefore short-lived. They have not had enough time to drift from the star-forming region before their death.

As discussed here and in Section 1.1 there are multiple possible progenitor paths for SNe IIn which may account for our observed multiple populations in NCR value.

4.1.1 *Type Ia-CSM and SN 2006gy*

As we have mentioned in Section 1.2.2, another scenario that may contribute to the SN IIn phenomenon are SNe Ia-CSM. SN Ia systems are old and will outlive their parent star formation region. Habergham et al. (2014) compares the NCR values of their sample of SNe IIn with other classes of SNe, including 98 SNe Ia. Just under 60% of the SNe Ia in that sample had a zero NCR value and most of the remainder were of lower NCR values, the slope on the cumulative frequency plot flattens out after around an NCR value of 0.600. The mean NCR value of the SNe Ia in Habergham et al. is 0.157. SNe Ia have mostly low or zero NCR values, therefore, SNe Ia-CSM may account for some of the zero and low NCR value SNe IIn in our sample.

A distinction between core-collapse SNe IIn and SNe Ia-CSM would not be directly picked up by the selection criteria set out by RHD21 as the classification system uses only the Hα line profile and

would require the transient to be a recognised SN Ia-CSM. In this study we have two possible SN Ia-CSM, SN 2006gy and SN 2008J for which we have continuum subtracted Hα data. However, we find that SN 2008J has an NCR value of 0.808 and SN 2006gy has a very high NCR value of 0.907, indicating these transients are in a strong, active star forming region. Alternatively to the thermonuclear origin of SN 2006gy, this transient may have a massive progenitor. For example, Smith et al. (2010) suggest that the $\sim 20\,M_\odot$ of CSM required a very high mass progenitor with mass $\sim 100\,M_\odot$. As most SNe Ia are not associated with Hα emission (Anderson et al. 2012; Habergham et al. 2014) this is unusual but one of the SNe Ia in the previous studies was in a region with an NCR value of over 0.900. As the thermonuclear origin of some of these transients becomes apparent at later times such as with SN 2006gy, it is possible that some of the transients in our sample would be made up of hitherto unknown SNe Ia-CSM. These could therefore make up some of the zero and low NCR value SNe IIn, assuming that SNe Ia-CSM are in similar environments to SNe Ia. However, Silverman et al. (2013) investigated 16 SNe Ia-CSM and found that all of them were found in spiral galaxies, suggesting that SNe Ia-CSM generally occur in younger populations when regular SNe Ia occur in all Hubble types (with some SN Ia subtypes preferring elliptical galaxies, see Hakobyan et al. 2020). Therefore, SNe Ia-CSM may, on average, have higher NCR values than regular SNe Ia (for example those in Anderson et al. 2012; Habergham et al. 2014). As the CSM may be created by a super-AGB companion, it is possible that SNe Ia-CSM may have a similar average NCR value to SNe IIP or ecSNe as discussed in Section 4.1.2. SNe Ia-CSM are rare (Graham et al. 2019a) and for example, out of 127 SNe Ia observed by ZTF, only one was observed to be a SN Ia-CSM (Yao et al. 2019). This rate may be overstated as SNe Ia-CSM are more luminous than SNe Ia, thus more easily observed. Due to the rarity of CSM interaction in SNe Ia, they likely do not make up a large "hidden" proportion of our SNe IIn sample, despite being the most numerous observed SN class (Li et al. 2011). On the other hand, a number of SNe Ia show late time CSM interaction, such as SN 2015cp that showed CSM interaction 664 days post-explosion (Graham et al. 2019b) so some SNe Ia may be unrecognised as SNe Ia-CSM if they lack late time observations.

4.1.2 *Electron-capture supernovae and SN 2008S*

Cai et al. (2021) examine the intermediate luminous red transient (ILRT) phenomenon and the possible connection to ecSNe. It was found that all five of these ILRTs resembled SN 2008S (which as well as being a prototypical impostor/transitional impostor to SN IIn is also considered a prototypical ILRT). The spectra show SN IIn-like narrow components to the Hα profiles so would be classified as SNe IIn by RHD21. The NCR value of SN 2008S was zero and ILRTs could make up a zero or low NCR value population of SNe IIn. SN 2008S exploded in a dusty environment. Habergham et al. (2014) cross-referenced 2MASS data of the hosts in their sample and found there was no underlying Hα region that was being obscured by a dusty environment.

Another example of a possible SN IIn with ecSN origin that is in our sample is SN 2015bf. This object has an NCR value of 0.657, which indicates a moderately strong region of ongoing star-formation. This contrasts with the zero NCR value of SN 2008S. Lin et al. (2021) present a study on SN 2015bf, they find that the spectrum evolves into a more standard SN II spectrum. SN 2015bf had a fairly high peak luminosity of -18 but the light curve then started to decay rapidly with a similar light curve morphology to other fast-declining SN II, including the ecSN candidate, SN 2018zd. Those authors argue that the brief CSM interaction seen in the spectral evolution points towards the CSM being fairly confined. This was interpreted as a violent mass loss episode shortly before the SN explosion. As ecSNe are expected to have progenitors on the low end of the progenitor mass range for CCSNe, they would be lower down the NCR value mass ladder. SN 2015bf eventually evolved as a SN II and Anderson et al. (2012) found that around 30% of SNe II had zero NCR values. Furthermore around 75% of these SNe had an NCR value under 0.500, so SNe IIn from ecSNe may make up some of our lower or zero NCR population.

4.1.3 *Mass-loss continuum*

SNe from lower mass progenitors such as ecSNe exemplify that mass loss sufficient to create enough CSM to produce the SN IIn phenomenon can be experienced by progenitors on the lower mass range for CCSNe. SNe IIn from lower mass progenitors such as RSGs may be classified as SNe IIn-P (SNe IIn with SN IIP-like light curves, e.g. SN 2013fs and PTF 11iqb Bullivant et al. 2018; Smith et al. 2015) or SNe IIn-L (SNe IIn with SN IIL-like light curves, e.g. SN 2013fr and SN 1998S Bullivant et al. 2018; Taddia et al. 2015).

In this work we find five examples of possible ecSNe: SN 2011ht (Roming et al. 2011), SN 1994W (Sollerman et al. 1998), SN 2009kn (Kankare et al. 2012), SN 2008S (Botticella et al. 2009) and SN 2015bf (Lin et al. 2021). All but one (SN 2015bf) have an NCR value of zero. This may be consistent with these objects having lower mass progenitors. Furthermore, the NCR distribution of standard SN II in Anderson et al. (2012) finds half the SNe in zero NCR regions.

Boian & Groh (2020) model early time spectra of SNe that exhibit early time CSM interaction. Boian & Groh use these models to explore the possible progenitors of 17 SNe with early time interaction. A wide range of SN parameters were calculated for this sample along with finding that there was increased mass loss immediately preceding the SN explosions. This early time interaction is not exclusive to the classic SN IIn class however, as, for example flash spectrum SNe also exhibit this behaviour and may have RSG progenitors (Khazov et al. 2016; Dessart et al. 2017; Kochanek 2019). Using the classification criteria in RHD21, it is possible that some of the silver class SNe IIn that have a limited number of spectra are actually flash spectrum SNe but further data is needed to demote these objects from silver SNe IIn.

4.2 SN 2005ip and long-lasting SNe IIn

A sub-category of SNe IIn are the long lasting SNe IIn. Examples of this phenomenon include SN 1988Z Turatto et al. (1993); Chugai & Danziger (1994), SN 1995G (Pastorello et al. 2002; Chugai & Danziger 2003), SN 2005ip (Stritzinger et al. 2012; Habergham et al. 2014; Smith et al. 2016), SN 2015da (Tartaglia et al. 2020), and KISS15s (Kokubo et al. 2019).

SN 2005ip is perhaps the most well studied long-lasting SN IIn. Habergham et al. (2014) found that SN 2005ip was still the brightest Hα source in its host, three years post explosion. Fox et al. (2020) present a study on SN 2005ip, including (very) late time photometry and find that SN 2005ip had only just started to decline in 2015. We find that SN 2005ip is no longer the strongest Hα source in the host with an NCR value of 0.866. However we do not include SN 2005ip in our analysis as we do not know whether the transient has dimmed to quiescent levels. Another example of a long-lasting SN IIn in our

sample is SN 2015da. Tartaglia et al. (2020) found that SN 2015da was still slowly declining four years post-explosion. Those authors suggest that the slow decline was due to ongoing CSM interaction with a CSM mass of $\sim 8\,M_\odot$ with an extreme pre-explosion mass loss rate of $\sim 0.6\,M_\odot\,yr^{-1}$. SN 2015da has a NCR value of 0.997, indicating that SN 2015da is in one of the strongest Hα emission regions in the host. This very high NCR value may be skewed by the ongoing interaction and is therefore not included in the NCR analysis. We do not find any additional examples of long-lasting SNe IIn in our observations.

4.3 SN 2009ip and precursors

Ofek et al. (2014); Strotjohann et al. (2021) found that many SNe IIn suffer from precursor explosions which may be LBV-like great eruptions. Notable examples include SN 2009ip (Foley et al. 2011; Mauerhan et al. 2013; Pastorello et al. 2013), SN 2011ht (Roming et al. 2011), and SN 2015bh (Boian & Groh 2018; Thöne et al. 2017).

We find that SN 2009ip is a very isolated transient, with an NCR value of zero and the similar transients, SN 2015bh and SN 2011ht were also zero NCR SNe IIn. If these precursor "impostor" events are LBV eruptions, these could be further examples of LBV isolation, possibly showing the effects of binary evolution.

In some cases there is little pre-explosion data. Groh et al. (2013a) suggest that if the archival images of the progenitor of SN 2005gl were taken at the time the progenitor was suffering a pre-SN IIn outburst, then the mass estimates for the progenitor may be overestimated. If this were the case, the progenitor may have a mass of around 20-25$M_\odot$.

SN impostors are an important consideration, and we can not rule out there being contamination in our sample (especially in the case of the silver SNe IIn). An environmental study of this nature, with a sample of SN impostors is difficult due to selection effects involved. Impostors are generally dim events so we may be biased towards exceptional, bright objects, especially if the objects are superimposed on a bright H II region. A study of the environments of SN impostors is therefore beyond the scope of this paper.

4.4 Radial distributions

We adopted the radial analysis used in Anderson & James (2009) and later in other studies (Habergham et al. 2012, 2014) in which the spatial distribution of our transients is compared with respect to younger stellar populations (traced by the Hα emission) and an older population (traced by the r'-band emission). Our findings were consistent with previous studies (e.g., in Habergham et al. 2014). In terms of the Hα emission, spatially, there may be a weak central concentration of SNe IIn shown by a possible peak in lower Fr(Hα) values. There may be a peak in intermediate Fr(R) values and a slight decline in frequency at higher Fr(R) values, indicating a dearth of SNe at the periphery of the host r'-band flux. The peak at intermediate values in the Fr(R) distribution may correspond with the possible central concentration in the Fr(Hα) as there tends to be less Hα emission in the central regions of galaxies so a low Fr(Hα) value may be further into the disc and in the mid-values of Fr(R).

We did not find a central excess in the radial distributions of SNe IIn. This does not follow the distributions seen for high mass (and high mass loss) progenitors such as those of SNe Ic. SNe Ic tend to be centrally located (van den Bergh 1997; Habergham et al. 2012) and as the radial distribution is a proxy for metallicity, are in higher metallicity environments.

We did not include SN impostors in this work. When Habergham et al. (2014) included impostors in their study, they found that the Fr(Hα) distribution had a peak at high values. This indicated that the impostors tended to be at the periphery of the host Hα emission. If many of the impostors are great eruptions of LBVs, then this would be consistent with the apparent isolation of LBVs we discussed in Section 4.1. The authors also found that there was a dearth of SNe in the central regions with very central SNe with respect to Fr(R), however do find central transients. Spatially there are a number of very central SNe IIn in our sample and RHD21 verified that these transients were not AGN.

4.5 Selection effects and detection sensitivity

We collated our sample from online databases which compile transients from many sources which include surveys that may be targeted or untargeted. Any bias inherent in these surveys will persist through to our target list. For example, large surveys such as the Zwicky Transient Survey (ZTF, Bellm et al. 2019) may introduce bias when transients are selected for spectroscopic followup.

The NCR method may lead to missing low level Hα emission. As the zero NCR population are the SNe where the cumulative sum is under zero, there may be a skew towards the positive pixel values and negative values, indicating that the low level emission is being missed. Therefore, we may be overestimating the zero NCR population. This could be remedied with larger telescopes with capabilities to perform deeper observations.

Another potential source of bias in our work is that we exclude hosts with smaller angular diameters from the radial distribution analysis.

4.6 Summary

We have presented the results of the largest environmental study of SN IIn hosts to date with 77 SNe IIn with most having a strong spectral classification. Our conclusions can be summarised as:

(i) We found that as a whole, SNe IIn do not follow star-formation as traced by Hα emission.
(ii) We find that around **40%** of SNe IIn are not associated with any SN IIn emission as calculated by NCR.
(iii) The non-zero NCR population is consistent with the hypothetical star-formation following population.
(iv) Our findings suggest there may be multiple progenitor routes to SNe IIn (e.g. ecSNe or SNe Ia-CSM). We do not see bimodality in our NCR distributions but we see multimodality in the full sample and non-zero NCR value subsample.
(v) There are no significant differences in the NCR distributions of the gold and silver classes. This suggests that many of the silver SNe IIn may be promoted to gold SNe IIn given more spectra.
(vi) The radial distributions of SNe IIn in terms of the r'-band and Hα emission is even. However we do note there are more centrally located SNe IIn than previous studies. While there is no central excess found in the distribution, there may be some SNe IIn progenitors that are similar to the progenitors of the massive, centrally concentrated SNe Ic.

Future surveys will provide a huge amount of data and transient discoveries. Surveys such as the ZTF and the Legacy Survey of Space and Time (LSST) at the Vera C. Rubin Observatory (LSST Science Collaboration et al. 2009) will provide a wealth of SN IIn candidates and will allow much larger samples to be used for constraining possible SN IIn progenitors.

ACKNOWLEDGEMENTS

We would like to thank the anonymous referee for their helpful and insightful comments. The Liverpool Telescope is operated on the island of La Palma by Liverpool John Moores University in the Spanish Observatorio del Roque de los Muchachos of the Instituto de Astrofisica de Canarias with financial support from the UK Science and Technology Facilities Council (STFC). This work makes use of observations from the Las Cumbres Observatory global telescope network. C.L.R. acknowledges a PhD studentship from STFC. S.M.H.-M. and M.J.D. acknowledge partial funding from STFC. The Isaac Newton Telescope and its service programme are operated on the island of La Palma by the Isaac Newton Group of Telescopes in the Spanish Observatorio del Roque de los Muchachos of the Instituto de Astrofísica de Canarias.

DATA AVAILABILITY

The data used in this work will be shared upon reasonable request to the author.

REFERENCES

Adams S. M., Kochanek C. S., Prieto J. L., Dai X., Shappee B. J., Stanek K. Z., 2016, MNRAS, 460, 1645
Aghakhanloo M., Murphy J. W., Smith N., Hložek R., 2017, MNRAS, 472, 591
Aldering G., et al., 2006, ApJ, 650, 510
Anderson T. W., Darling D. A., 1952, The Annals of Mathematical Statistics, 23, 193
Anderson J. P., James P. A., 2008, MNRAS, 390, 1527
Anderson J. P., James P. A., 2009, MNRAS, 399, 559
Anderson J. P., Habergham S. M., James P. A., Hamuy M., 2012, MNRAS, 424, 1372
Arbour R., 2008, Central Bureau Electronic Telegrams, 1235, 2
Barnsley R. M., Jermak H. E., Steele I. A., Smith R. J., Bates S. D., Mottram C. J., 2016, Journal of Astronomical Telescopes, Instruments, and Systems, 2, 015002
Beasor E. R., Davies B., Smith N., van Loon J. T., Gehrz R. D., Figer D. F., 2020, MNRAS, 492, 5994
Bellm E. C., et al., 2019, PASP, 131, 018002
Boian I., Groh J. H., 2018, Astronomy & Astrophysics, 617, A115
Boian I., Groh J. H., 2020, MNRAS, 496, 1325
Botticella M. T., et al., 2009, MNRAS, 398, 1041
Brennan S. J., et al., 2021a, arXiv e-prints, p. arXiv:2102.09572
Brennan S. J., et al., 2021b, arXiv e-prints, p. arXiv:2102.09576
Brown T. M., et al., 2013, PASP, 125, 1031
Bullivant C., et al., 2018, MNRAS, 476, 1497
Cai Y. Z., et al., 2021, A&A, 654, A157
Chugai N. N., 1991, MNRAS, 250, 513
Chugai N. N., 2001, MNRAS, 326, 1448
Chugai N. N., Danziger I. J., 1994, MNRAS, 268, 173
Chugai N. N., Danziger I. J., 2003, Astronomy Letters, 29, 649
Chugai N. N., et al., 2004, Monthly Notices of the Royal Astronomical Society, 352, 1213
Deng J., et al., 2004, The Astrophysical Journal, 605, L37
Dessart L., Hillier D. J., Gezari S., Basa S., Matheson T., 2009, MNRAS, 394, 21
Dessart L., John Hillier D., Audit E., 2017, A&A, 605, A83
Dilday B., et al., 2012, Science, 337, 942
Duyvendak J. J. L., 1942, PASP, 54, 91
Dwarkadas V. V., 2011, MNRAS, 412, 1639
Earl N., et al., 2022, astropy/specutils: V1.6.0, doi:10.5281/zenodo.5911360, https://doi.org/10.5281/zenodo.5911360
Elias-Rosa N., et al., 2018, MNRAS, 475, 2614
Evans C. J., Lennon D. J., Smartt S. J., Trundle C., 2006, A&A, 456, 623
Filippenko A. V., 1989, AJ, 97, 726
Filippenko A. V., 1997, ARA&A, 35, 309
Foley R. J., Berger E., Fox O., Levesque E. M., Challis P. J., Ivans I. I., Rhoads J. E., Soderberg A. M., 2011, The Astrophysical Journal, 732, 32
Fox O. D., et al., 2020, MNRAS, 498, 517
Fraser M., et al., 2013, MNRAS, 433, 1312
Fraser M., et al., 2015, MNRAS, 453, 3886
Gal-Yam A., et al., 2007, ApJ, 656, 372
Gangopadhyay A., et al., 2020, Monthly Notices of the Royal Astronomical Society, 499, 129
García B., Mermilliod J. C., 2001, A&A, 368, 122
Georgy C., Meynet G., Walder R., Folini D., Maeder A., 2009, A&A, 502, 611
Germany L. M., Reiss D. J., Sadler E. M., Schmidt B. P., Stubbs C. W., 2000, The Astrophysical Journal, 533, 320
Gies D. R., 1987, ApJS, 64, 545
Graham M. L., et al., 2017, Monthly Notices of the Royal Astronomical Society, 469, 1559
Graham M. L., et al., 2019a, ApJ, 871, 62
Graham M. L., et al., 2019b, The Astrophysical Journal, 871, 62
Groh J. H., Meynet G., Ekström S., 2013a, A&A, 550, L7
Groh J. H., Georgy C., Ekström S., 2013b, A&A, 558, L1
Habergham S. M., James P. A., Anderson J. P., 2012, MNRAS, 424, 2841
Habergham S. M., Anderson J. P., James P. A., Lyman J. D., 2014, MNRAS, 441, 2230
Hakobyan A. A., Barkhudaryan L. V., Karapetyan A. G., Gevorgyan M. H., Mamon G. A., Kunth D., Adibekyan V., Turatto M., 2020, MNRAS, 499, 1424
Hamuy M., Phillips M., Suntzeff N., Maza J., 2003, International Astronomical Union Circular, 8151, 2
Hartigan J. A., Hartigan P. M., 1985, The Annals of Statistics, 13, 70
Haydon D. T., Kruijssen J. M. D., Hygate A. e. P. S., Schruba A., Krumholz M. R., Chevance M., Longmore S. N., 2018, arXiv e-prints, p. arXiv:1810.10897
Haydon D. T., Kruijssen J. M. D., Chevance M., Hygate A. P. S., Krumholz M. R., Schruba A., Longmore S. N., 2020, MNRAS, 498, 235
Helou G., Madore B., 1988, in European Southern Observatory Conference and Workshop Proceedings. pp 335–340
Henry R., Worthey G., 1999, Publications of the Astronomical Society of the Pacific, 111, 919
Huang C., Chevalier R. A., 2018, MNRAS, 475, 1261
Humphreys R. M., Davidson K., 1994, PASP, 106, 1025
Humphreys R. M., Davidson K., Jones T. J., Pogge R. W., Grammer S. H., Prieto J. L., Pritchard T. A., 2012, ApJ, 760, 93
Humphreys R. M., Davidson K., Gordon M. S., Weis K., Burggraf B., Bomans D. J., Martin J. C., 2014, ApJ, 782, L21
Humphreys R. M., Weis K., Davidson K., Gordon M. S., 2016, ApJ, 825, 64
Humphreys R. M., Davidson K., Van Dyk S. D., Gordon M. S., 2017, ApJ, 848, 86
Institute S., 1989, SAS Institute Inc., Cary, NC
James P. A., Anderson J. P., 2006, A&A, 453, 57
Jerkstrand A., Maeda K., Kawabata K. S., 2020, Science, 367, 415
Kangas T., Mattila S., Kankare E., Kotilainen J. K., Väisänen P., Greimel R., Takalo A., 2013, MNRAS, 436, 3464
Kangas T., et al., 2017, A&A, 597, A92
Kankare E., et al., 2012, MNRAS, 424, 855
Kankare E., et al., 2015, A&A, 581, L4
Kasliwal M. M., Cenko S. B., Kulkarni S. R., Ofek E. O., Quimby R., Rau A., 2011, ApJ, 735, 94
Kasliwal M. M., Kulkarni S. R., Gal-Yam A., Nugent P. E., Sullivan M., Bildsten L., Yaron O., Perets H. B., 2012, ApJ, 755, 161
Khazov D., et al., 2016, ApJ, 818, 3
Kiewe M., et al., 2012, ApJ, 744, 10
Kochanek C. S., 2019, MNRAS, 483, 3762
Kochanek C. S., Szczygieł D. M., Stanek K. Z., 2012, ApJ, 758, 142
Kokubo M., et al., 2019, The Astrophysical Journal, 872, 135
Kuncarayakti H., et al., 2013, AJ, 146, 31

LSST Science Collaboration et al., 2009, arXiv e-prints, p. arXiv:0912.0201
Law N. M., et al., 2009, Publications of the Astronomical Society of the Pacific, 121, 1395
Li W., et al., 2011, MNRAS, 412, 1441
Lin H., et al., 2021, MNRAS, 505, 4890
Maeder A., Meynet G., 2008, in de Koter A., Smith L. J., Waters L. B. F. M., eds, Astronomical Society of the Pacific Conference Series Vol. 388, Mass Loss from Stars and the Evolution of Stellar Clusters. p. 3
Martin C., et al., 2003, in Blades J. C., Siegmund O. H. W., eds, Proc. SPIEVol. 4854, Future EUV/UV and Visible Space Astrophysics Missions and Instrumentation.. pp 336–350, doi:10.1117/12.460034
Mauerhan J., Smith N., 2012, MNRAS, 424, 2659
Mauerhan J. C., et al., 2013, Monthly Notices of the Royal Astronomical Society, 430, 1801
Mayall N. U., Oort J. H., 1942, PASP, 54, 95
Meikle P., Fassia A., Geballe T. R., Lundqvist P., Chugai N., Farrah D., Sollerman J., 2003, in Hillebrandt W., Leibundgut B., eds, From Twilight to Highlight: The Physics of Supernovae. p. 229 (arXiv:astro-ph/0211144), doi:10.1007/10828549_30
Miyaji S., Nomoto K., Yokoi K., Sugimoto D., 1980, PASJ, 32, 303
Moriya T. J., Maeda K., Taddia F., Sollerman J., Blinnikov S. I., Sorokina E. I., 2014, Monthly Notices of the Royal Astronomical Society, 439, 2917–2926
Nomoto K., 1984, ApJ, 277, 791
Nomoto K., 1987, ApJ, 322, 206
Nyholm A., et al., 2020, Astronomy & Astrophysics, 637, A73
Ofek E. O., et al., 2007, The Astrophysical Journal, 659, L13
Ofek E. O., et al., 2013, Nature, 494, 65
Ofek E. O., et al., 2014, ApJ, 789, 104
Pastorello A., et al., 2002, MNRAS, 333, 27
Pastorello A., et al., 2013, The Astrophysical Journal, 767, 1
Pastorello A., et al., 2018, Monthly Notices of the Royal Astronomical Society, 474, 197–218
Pessi T., Prieto J. L., Monard B., Kochanek C. S., Bock G., Drake A. J., Fox O. D., Parker S., 2021, arXiv e-prints, p. arXiv:2110.09546
Pettini M., Pagel B. E. J., 2004, MNRAS, 348, L59
Prieto J., Garnavich P., Depoy D., Marshall J., Eastman J., Frank S., 2005, Central Bureau Electronic Telegrams, 302, 1
Prieto J. L., et al., 2008, ApJ, 681, L9
Ransome C. L., Habergham-Mawson S. M., Darnley M. J., James P. A., Filippenko A. V., Schlegel E. M., 2021, MNRAS, 506, 4715
Rau A., et al., 2009, PASP, 121, 1334
Roming P., Pritchard T., Brown P., 2011, The Astronomer's Telegram, 3690, 1
Schlegel E. M., 1990, MNRAS, 244, 269
Silverman J. M., et al., 2013, ApJS, 207, 3
Smith N., 2014, Annual Review of Astronomy and Astrophysics, 52, 487
Smith N., Tombleson R., 2014, Monthly Notices of the Royal Astronomical Society, 447, 598
Smith N., Gehrz R. D., Hinz P. M., Hoffmann W. F., Hora J. L., Mamajek E. E., Meyer M. R., 2003, AJ, 125, 1458
Smith N., et al., 2007, The Astrophysical Journal, 666, 1116
Smith N., Hinkle K. H., Ryde N., 2009, AJ, 137, 3558
Smith N., et al., 2010, AJ, 139, 1451
Smith N., Li W., Silverman J. M., Ganeshalingam M., Filippenko A. V., 2011, Monthly Notices of the Royal Astronomical Society, 415, 773
Smith N., Mauerhan J. C., Kasliwal M. M., Burgasser A. J., 2013, MNRAS, 434, 2721
Smith N., Mauerhan J. C., Prieto J. L., 2014, MNRAS, 438, 1191
Smith N., et al., 2015, Monthly Notices of the Royal Astronomical Society, 449, 1876–1896
Smith N., et al., 2016, MNRAS, 458, 950
Smith N., et al., 2017, MNRAS, 466, 3021
Smith N., et al., 2020, MNRAS, 492, 5897
Sollerman J., Cumming R. J., Lundqvist P., 1998, ApJ, 493, 933
Stathakis R. A., Sadler E. M., 1991, MNRAS, 250, 786
Steele T. N., Cobb B., Filippenko A. V., 2009, Central Bureau Electronic Telegrams, 2011, 1
Stephens M. A., 1974, Journal of the American Statistical Association, 69, 730
Stritzinger M., et al., 2012, ApJ, 756, 173
Strotjohann N. L., et al., 2021, ApJ, 907, 99
Taddia F., et al., 2013, A&A, 555, A10
Taddia F., et al., 2015, A&A, 580, A131
Tartaglia L., et al., 2020, A&A, 635, A39
The Astropy Collaboration Robitaille, Thomas P. Tollerud, Erik J. Greenfield, Perry Droettboom, Michael Bray, Erik Aldcroft, Tom Davis, Matt 2013, A&A, 558, A33
Thompson T. A., Prieto J. L., Stanek K. Z., Kistler M. D., Beacom J. F., Kochanek C. S., 2009, ApJ, 705, 1364
Thöne C. C., et al., 2017, A&A, 599, A129
Tody D., 1986, in Crawford D. L., ed., Society of Photo-Optical Instrumentation Engineers (SPIE) Conference Series Vol. 627, Instrumentation in astronomy VI. p. 733, doi:10.1117/12.968154
Turatto M., Cappellaro E., Danziger I. J., Benetti S., Gouiffes C., della Valle M., 1993, MNRAS, 262, 128
Weis K., Bomans D. J., 2020, Galaxies, 8, 20
Wenger M., et al., 2000, A&AS, 143, 9
Yao Y., et al., 2019, ApJ, 886, 152
Yaron O., et al., 2017, Nature Physics, 13, 510–517
de Jager C., 1998, A&ARv, 8, 145
van den Bergh S., 1997, AJ, 113, 197

This paper has been typeset from a TEX/LATEX file prepared by the author.